



Cite this: *Green Chem.*, 2025, **27**, 5359

Received 21st February 2025,  
Accepted 6th April 2025

DOI: 10.1039/d5gc00942a

rsc.li/greenchem

## Deoxygenative dual $\text{CO}_2$ conversions: methylation and switchable *N*-formylation/*N*-methylation of tryptamines†

Kazuto Takaishi, \* Hajime Morishita, Kosuke Iwaki and Tadashi Ema \*

The unprecedented one-pot synthesis of *N*-formyl/*N*-methyltryptolines from tryptamines was achieved via phenylsilane-assisted deoxygenative dual  $\text{CO}_2$  conversions. Two  $\text{CO}_2$  molecules acted as different synthons and were converted into methylene and *N*-formyl/*N*-methyl groups. The  $\text{CO}_2$  reduction step was catalyzed by a pentanuclear zinc complex at atmospheric pressure under solvent-free conditions. The *N*-formyl/*N*-methyl products could be switched by changing the amount of phenylsilane, and the amounts of *in situ* generated bis(silyl)acetals and silyl formates were key to the chemoselectivity. Methylenation, *N*-formylation, and *N*-methylation proceeded via the Pictet–Spengler reaction, amine–acid condensation, and the Eschweiler–Clarke reaction, respectively. The  $\text{CO}_2$  reduction with phenylsilane could also be applied to the one-pot three-step synthesis of spiro[oxindole–pyrrolidine]s.

### Green foundation

1. We have developed new types of deoxygenative dual  $\text{CO}_2$  conversions in which two  $\text{CO}_2$  molecules act as different synthons and are converted into methylene and *N*-formyl/*N*-methyl groups of tryptolines, known as important compounds in biology. These  $\text{CO}_2$  fixation methods will expand the usefulness of  $\text{CO}_2$ .
2. The  $\text{CO}_2$  conversions have been achieved under solvent-free conditions at atmospheric pressure. The  $\text{CO}_2$  reduction step was catalyzed by a small amount (0.07 mol%) of zinc complex, which could be prepared easily, and therefore noble and toxic metals are not required. Moreover,  $\text{H}_2\text{O}$  could be used as an additive.
3. Our methods could be made greener by catalyst reuse strategies in flow chemistry. In addition, methods that allow for the application of a variety of sustainable reductants are recommended.

## Introduction

$\text{CO}_2$  is a renewable C1 building block and is expected to serve as an alternative to petroleum-based chemicals. Therefore, the development of fine organic synthetic methods with  $\text{CO}_2$  for value-added chemicals has become increasingly important.<sup>1</sup> Among  $\text{CO}_2$  fixations, deoxygenative conversions involving C–H/C–C bond formation, such as conversion to methyl ( $-\text{CH}_3$ )<sup>2</sup> or methylene ( $-\text{CH}_2-$ )<sup>3</sup> groups, are still rare despite their importance. Deoxygenative  $\text{CO}_2$  conversions require reductants, and  $\text{H}_2$ ,<sup>4</sup> hydroboranes,<sup>5,6</sup> and hydrosilanes<sup>6,7</sup> are often used in the presence of catalysts. In the case of hydrosilanes, the reduction of  $\text{CO}_2$  generates reactive species: silyl formates ( $\text{HCO}_2\text{Si}$ ), bis(silyl)acetals ( $\text{SiOCH}_2\text{OSi}$ ), and methoxysilanes

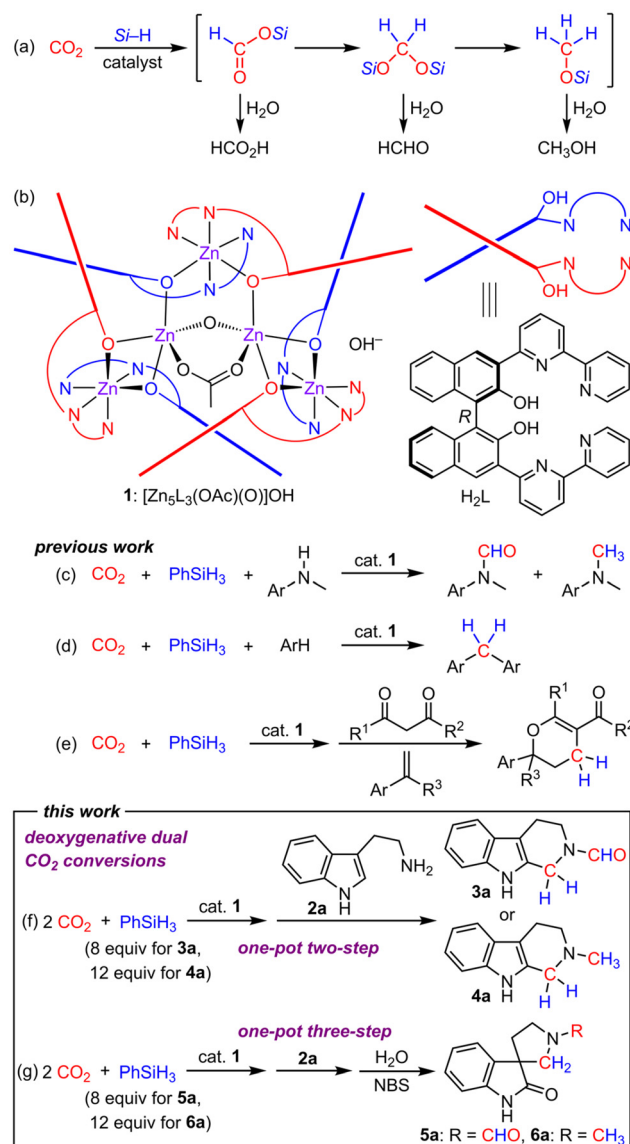
( $\text{CH}_3\text{OSi}$ ), which are easily hydrolyzed to formic acid, formaldehyde, and methanol, respectively (Scheme 1a). Among the silyl species, bis(silyl)acetals are potentially useful for C–H/C–C bond-forming reactions, but there are few reports.<sup>6</sup>

Double  $\text{CO}_2$  conversions, where two  $\text{CO}_2$  molecules are captured by one substrate molecule, are attractive molecular conversions. Although several double carboxylations have been reported,<sup>8</sup> the number of double deoxygenative  $\text{CO}_2$  conversions reported is severely limited. For example, the Yan–You-Jiang group reported the construction of a tetrahydropyrimidine ring in which two  $\text{CO}_2$  molecules were converted into two methylene groups,<sup>9</sup> and our group reported the construction of a fused benzene ring by conversion into two aromatic CH groups.<sup>10</sup> In contrast, the Qi–Jiang group reported the synthesis of  $\alpha$ -methyl- $\beta$ -diketones from aryl iodides, alkynes, and  $\text{CO}_2$ , where two  $\text{CO}_2$  molecules were transformed into two different moieties, carbonyl and methyl groups.<sup>11</sup> The Nan group has recently developed the synthesis of methyl-indoloquinoxalines from indolylanilines with  $\text{CO}_2$  via double *N*-formylation in which two  $\text{CO}_2$  molecules were converted into an aromatic carbon and a methyl group.<sup>12</sup> Such dual  $\text{CO}_2$  con-

Division of Applied Chemistry, Graduate School of Environmental, Life, Natural Science and Technology, Okayama University, Tsushima, Okayama 700-8530, Japan.  
E-mail: [takaishi@okayama-u.ac.jp](mailto:takaishi@okayama-u.ac.jp), [ema@cc.okayama-u.ac.jp](mailto:ema@cc.okayama-u.ac.jp)

† Electronic supplementary information (ESI) available. CCDC 2413450 and 2413452. For ESI and crystallographic data in CIF or other electronic format see DOI: <https://doi.org/10.1039/d5gc00942a>



Scheme 1  $\text{CO}_2$  fixation with  $\text{Zn}^{II}$  complex 1.

versions will expand the usefulness of  $\text{CO}_2$ , and the development of new types of conversions would be a highly valuable achievement.

We have previously reported a macrocyclic pentanuclear  $\text{Zn}^{II}$  complex 1, which can be easily prepared *via* the self-assembly of the binaphthyl-bipyridyl ligand  $\text{H}_2\text{L}$  and  $\text{Zn}(\text{OAc})_2 \cdot 2\text{H}_2\text{O}$  (Scheme 1b).<sup>13</sup> Complex 1 exhibited catalytic activity toward deoxygenative  $\text{CO}_2$  conversions *via* the hydro-silylation of  $\text{CO}_2$ ,<sup>14</sup> temperature-switched  $N$ -formylation/ $N$ -methylation of amines (Scheme 1c),<sup>13,15</sup>  $C$ -methylation of arenes (Scheme 1d),<sup>14a</sup> and the synthesis of 3,4-dihydropyrans from  $\beta$ -dicarbonyl compounds and styrenes (Scheme 1e).<sup>14b</sup>

More recently, during the investigation of the scope of 1-catalyzed  $\text{CO}_2$  fixation, we unexpectedly noticed that tryptamine (2a) was converted into 2-formyltryptoline (3a) (tryptoline is also known as 1,2,3,4-tetrahydro- $\beta$ -carboline), a novel com-

ound (Scheme 1f). In this synthesis, two  $\text{CO}_2$  molecules were incorporated into two different moieties, methylene and  $N$ -formyl groups, and this type of  $\text{CO}_2$  conversion is unprecedented. The Pictet-Spengler cyclization involving formaldehyde and amine-formic acid condensation seems to proceed. Tryptoline derivatives often exhibit pharmacological activities in the treatment of serious diseases such as mitochondrial disease, Alzheimer's disease, and malaria.<sup>16</sup> Therefore, expanding the synthetic methods of tryptolines would be a significant contribution, and we decided to investigate this synthesis. As a result, we established the synthetic conditions leading to 3a and found that the product could be switched to 2-methyltryptoline (4a). In addition, one-pot three-step reactions, Br-assisted semi-pinacol rearrangement<sup>17</sup> after the formation of 3a or 4a, proceeded to form spiro[oxindole-pyrrolidine]s 5a and 6a (Scheme 1g). Some derivatives with this spiro-skeleton also exhibit pharmaceutical activity,<sup>18</sup> and the method matches the pot-economy concept.<sup>19</sup> Therefore, this strategy is promising.

## Results and discussion

### Optimizing the reaction conditions

We first optimized the reaction conditions for the synthesis of formyltryptoline 3a from 2a (Table 1). After the reaction of  $\text{CO}_2$  (1 atm) with  $\text{PhSiH}_3$  (8 equiv.) in the presence of catalyst 1 (0.07 mol%) under solvent-free conditions, 2a was added along with additives  $\text{AcOH}$  and  $\text{H}_2\text{O}$  (entries 1–5). The yield was sen-

Table 1 Optimization of the reaction conditions<sup>a</sup>

Entry	X (equiv.)	$T_1$ (°C)	$T_2$ (°C)	Yield <sup>b</sup> (%)	
				3a	4a
1	8	45	100	38	5
2	8	55	100	62	8
3	8	65	100	49	12
4	8	55	120	83 (80) <sup>c</sup>	6
5	8	55	140	29	4
6 <sup>d</sup>	8	55	120	27	21
7 <sup>e</sup>	8	55	120	60	19
8	6	55	120	43	3
9	10	55	120	64	34
10	12	55	120	14	82 (83) <sup>c</sup>
11 <sup>f</sup>	14	55	120	4	82
12	14	55	120	Trace	76

<sup>a</sup> Conditions:  $\text{CO}_2$  (1 atm, balloon, 3.7 L),  $\text{PhSiH}_3$  (6–14 equiv.), cat. 1 (0.07 mol% based on  $\text{PhSiH}_3$ ), 2a (0.25 mmol),  $\text{AcOH}$  (200  $\mu\text{L}$ ),  $\text{H}_2\text{O}$  (100  $\mu\text{L}$ ). <sup>b</sup> Determined by  $^1\text{H}$  NMR using styrene as an internal standard. <sup>c</sup> Isolated yield. <sup>d</sup> Absence of  $\text{AcOH}$ . <sup>e</sup> Absence of  $\text{H}_2\text{O}$ . <sup>f</sup>  $\text{DMSO}$  (100  $\mu\text{L}$ ) was added.



sitive to temperature, and the optimal temperatures were 55 and 120 °C for the first and second steps, respectively (83%, entry 4).

In the first step, key C1 intermediates, bis(silyl)acetals and silyl formates, are considered to accumulate. When AcOH or H<sub>2</sub>O was absent, the yields decreased (27–60%, entries 6 and 7). We also screened hydrosilanes and additives, which resulted in lower yields (Tables S1–S4†). We noticed that methyltryptoline **4a** was generated as a byproduct (4–21%, entries 1–7) and changed the amount of PhSiH<sub>3</sub> to increase

the yield of **4a** (entries 8–12). Compound **4a** was formed in the highest yield (82%, entry 10) when 12 equiv. of PhSiH<sub>3</sub> were used. The addition of DMSO did not improve the yield (entry 11). On the basis of the above results, entries 4 and 10 were found to be the best conditions for the synthesis of **3a** and **4a**, respectively. The structures of **3a** and **4a** were unambiguously confirmed by X-ray crystallography (Fig. 1 and S2†).<sup>20</sup>

### Substrate scope

We next investigated the substrate scope for the chemoselective dual CO<sub>2</sub> conversions (Scheme 2). When 5-methyl-, 5-methoxy-, 5-bromo-, 7-methyl-, 1-methyl-, and 1-ethyl-substituted tryptamines were used as substrates, the corresponding formyltryptolines **3b–3g** (51–78%) and methyltryptolines **4b–4g** (46–74%) were obtained selectively in moderate to high yields, depending on the amount of phenylsilane. Moreover, 1-benzyl-, 1-(4-methoxybenzyl)-, and 1-(4-chlorobenzyl)-substituted tryptamines were also converted into formyltryptolines **3h–3j** (45–84%) or methyltryptolines **4h–4j** (55–89%) in gratifying

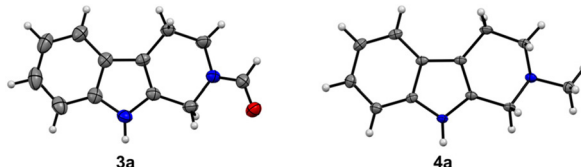
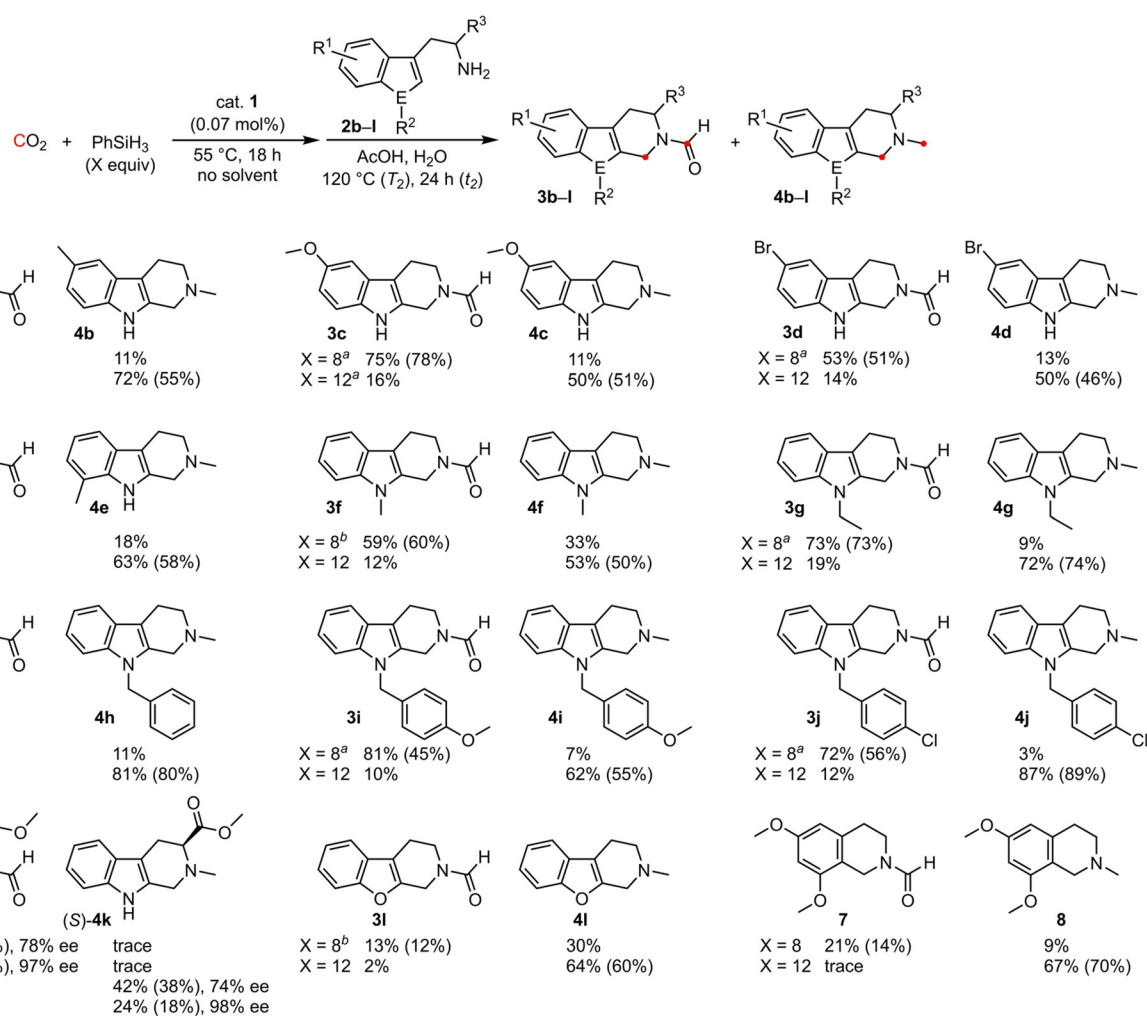


Fig. 1 ORTEP drawings of X-ray crystal structures of **3a** and **4a**. The thermal ellipsoids are scaled to the 50% probability level.



Scheme 2 Substrate scope. Yields were determined by <sup>1</sup>H NMR using styrene as an internal standard. Isolated yields are shown in parentheses. <sup>a</sup> T<sub>2</sub> = 130 °C. <sup>b</sup> T<sub>2</sub> = 110 °C. <sup>c</sup> T<sub>2</sub> = 90 °C. <sup>d</sup> T<sub>2</sub> = 80 °C, t<sub>2</sub> = 3 h. <sup>e</sup> T<sub>2</sub> = 45 °C.



yields despite the large steric hindrance. The fact that even 1-substituted tryptamines underwent the reactions demonstrates the usefulness of this synthetic method. In addition, (*S*)-tryptophan methyl ester could be transformed into (*S*)-**3k** (26%, 78% ee at  $T_2$  of 130 °C) or (*S*)-**4k** (38%, 74% ee at  $T_2$  of 80 °C) although partial racemization proceeded. The racemization could be suppressed to a minimum by lowering the reaction temperature ((*S*)-**3k**: 17%, 97% ee at  $T_2$  of 90 °C; (*S*)-**4k**: 18%, 98% ee at  $T_2$  of 45 °C). For the scope of substrates beyond tryptamines, benzofuran and dimethoxybenzene analogs were converted into methylated tetrahydrobenzofuropyridine **4l** (60%) and tetrahydroisoquinoline **8** (70%), respectively, in gratifying yields, although the yields of formylated products were low. The aforementioned results indicate that the substrate scope is relatively broad.

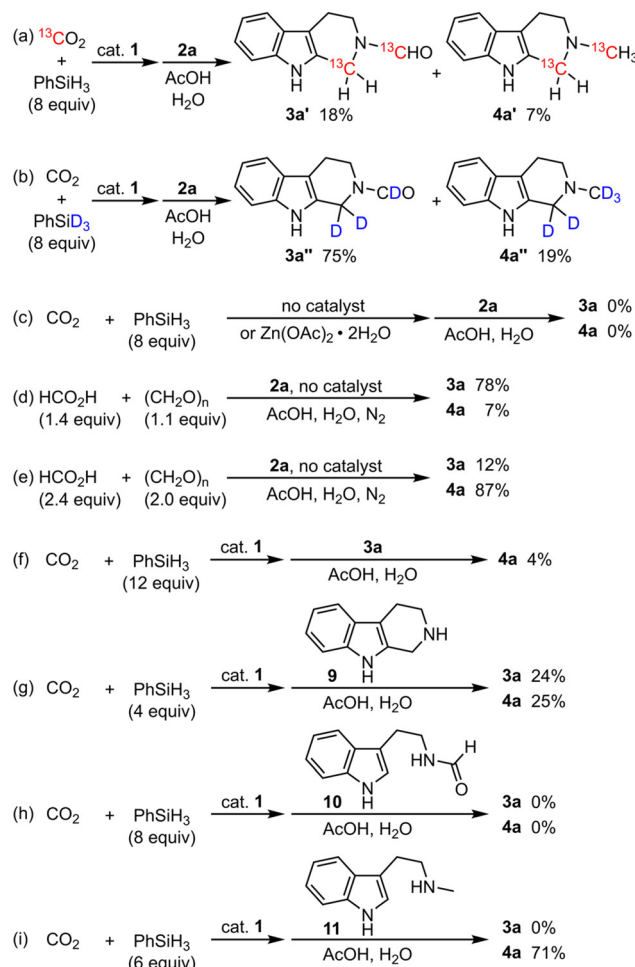
### Isotope-labeling and control experiments

To elucidate the carbon and hydrogen sources for the construction of **3a** and **4a**, isotope-labeling experiments were conducted. When the reaction was performed with  $^{13}\text{CO}_2$ , **3a'** possessing one each of  $^{13}\text{C}$ -methylene and  $^{13}\text{C}$ -formyl groups and **4a'** possessing one each of  $^{13}\text{C}$ -methylene and  $^{13}\text{C}$ -methyl groups were obtained without the formation of **3a** and **4a** (Scheme 3a).<sup>21</sup> When the reaction was performed with  $\text{PhSiD}_3$ , **3a''** possessing deuterated methylene and formyl groups and **4a''** possessing deuterated methylene and methyl groups were obtained without the formation of **3a** and **4a** (Scheme 3b). These results clearly demonstrate that the incorporated carbon and hydrogen atoms originated from carbon dioxide and phenylsilane, respectively.

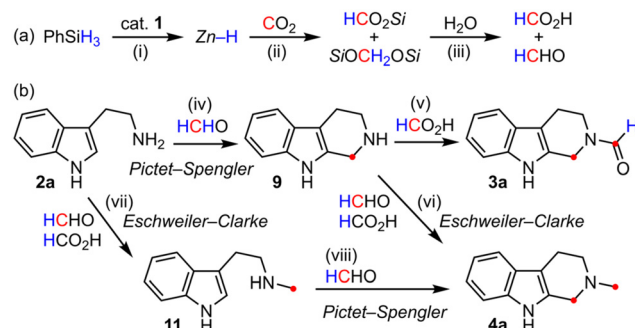
We performed control experiments to predict the reaction mechanisms. An experiment without catalyst **1** resulted in no formation of **3a** or **4a**, and  $\text{Zn}(\text{OAc})_2 \cdot 2\text{H}_2\text{O}$  showed no catalytic activity, both indicating that **1** is an essential catalyst (Scheme 3c). When formic acid and paraformaldehyde were used instead of  $\text{CO}_2$  and  $\text{PhSiH}_3$ , **3a** or **4a** was obtained selectively according to the amounts of reagents (Scheme 3d and e).<sup>22</sup> In contrast, the reactions did not proceed with paraformaldehyde or formic acid alone (not shown), which strongly suggests that the system requires both paraformaldehyde and formic acid (or their equivalents) as intermediates. When **3a** was used as a substrate, **4a** was hardly obtained, which indicates that **3a** is not a major intermediate leading to **4a** (Scheme 3f). When tryptoline (**9**) was used as a substrate, both **3a** and **4a** were obtained, indicating that **9** is a common intermediate (Scheme 3g). In contrast, formyltryptamine **10** did not give **3a**, suggesting that **10** is not an intermediate and that the electron-withdrawing formyl group prevents the Pictet–Spengler cyclization (Scheme 3h). On the other hand, methyltryptamine **11** afforded **4a**, which indicates that **11** as well as **9** is an intermediate for **4a** (Scheme 3i).

### Proposed pathways

The above isotope-labeling and control experiments enabled us to propose the following pathways (Scheme 4). First, (i–ii)



**Scheme 3** Isotope-labeling and control experiments.



**Scheme 4** Proposed pathways for the synthesis of **3a** and **4a**.

$\text{PhSiH}_3$  via the formation of a  $\text{Zn}$ –hydride complex, and (iii) subsequent hydrolysis gives formic acid and formaldehyde (Scheme 4a).<sup>13</sup> Next, (iv) the Pictet–Spengler reaction<sup>3d,e</sup> of **2a** with formaldehyde affords **9**, and (v) the formylation with formic acid gives **3a** (Scheme 4b). Instead of this formylation, (vi) the Eschweiler–Clarke reaction with formaldehyde and formic acid gives **4a**. As for the synthesis of **4a**, another route is possible: (vii) the Eschweiler–Clarke reaction of **2a** to form



11 and (viii) the subsequent Pictet–Spengler reaction. Because 3a could be generated enough experimentally, it is supposed that reaction (iv) is faster than reaction (vii) and that the route *via* 9 is the main pathway for the synthesis of 4a. Here, 9 was not detected experimentally even when the reaction time was shortened, which indicates that reaction (iv) includes the rate-determining step.

### Chemoselectivity in the formation of 3a or 4a

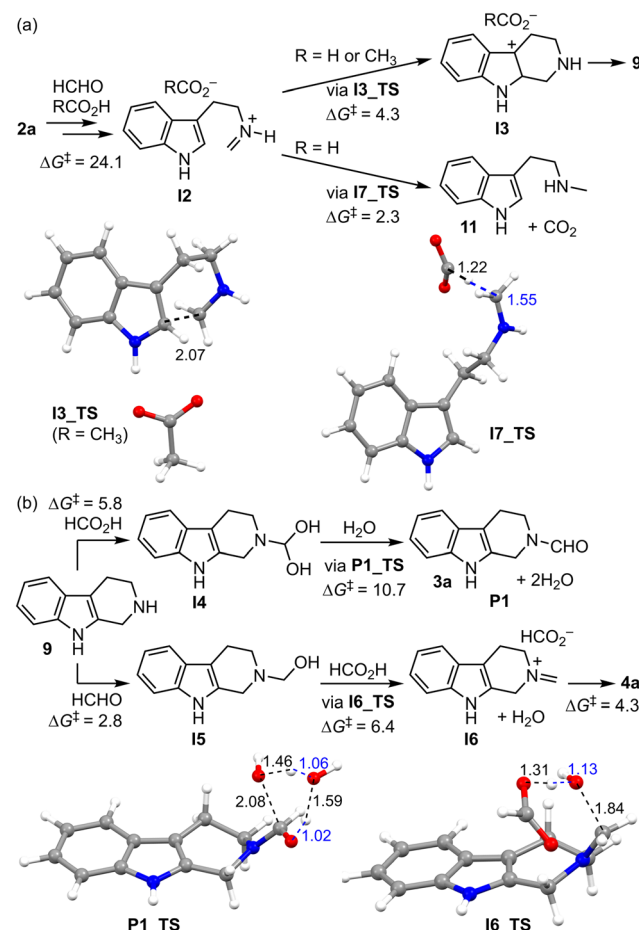
We next turned our attention to the origin of the chemoselectivity in the formation of 3a or 4a. The amounts and/or molar ratio of C1 intermediates generated in the first step (CO<sub>2</sub> reduction step) were strongly expected to depend on the amount of PhSiH<sub>3</sub>, which could be considered a determinant of the selectivity. Therefore, we measured their amounts in the reaction mixtures from the first step under the standard conditions (Table 2 and Fig. S6†).<sup>23</sup> When 2.00 mmol of PhSiH<sub>3</sub> (for the synthesis of 3a) was used, 0.46 mmol of silyl formates and 0.35 mmol of bis(silyl)acetals were detected together with methoxysilanes. When 3.00 mmol of PhSiH<sub>3</sub> (for the synthesis of 4a) was used, 0.73 mmol of silyl formates and 0.60 mmol of bis(silyl)acetals were detected. Although the quantities changed, the proportions were remarkably similar: 30% for silyl formates, 25% for bis(silyl)acetals, and 45% for methoxysilanes. In other words, the amounts, not the ratio, of C1 intermediates determine the main product. In the case that an amount of bis(silyl)acetals is small, generated formaldehyde is depleted in the Pictet–Spengler reaction of 2a and cannot participate in the subsequent Eschweiler–Clarke reaction; thus, N-formylation proceeds selectively to give 3a. In the case that a sufficient amount of bis(silyl)acetals is accumulated, 4a forms selectively because the Eschweiler–Clarke reaction of 9 is faster than the N-formylation.

To more reliably elucidate the pathways and chemoselectivity, we carried out DFT calculations. Selected elementary reactions and overall pathways with energy profiles are shown in Scheme 5 and S2–S4,† respectively. As a result, the pathways shown in Scheme 4b are acceptable, and some highlights are as follows. Iminium salt I2 is formed from 2a as a common intermediate *via* a rate-determining dehydration step with a  $\Delta G^\ddagger$  value of 24.1 kcal mol<sup>−1</sup> (Scheme 5a). Then, I2 branches into the reactions to I3 (for 9) and 11, and the  $\Delta G^\ddagger$  value of the transition state (TS) to I3 (4.3 kcal mol<sup>−1</sup>) is slightly greater than that to 11 (2.3 kcal mol<sup>−1</sup>). Here, it should

Table 2 CO<sub>2</sub> reduction with PhSiH<sub>3</sub><sup>a</sup>

PhSiH <sub>3</sub> (mmol)	Production amount <sup>b</sup> (mmol)		
	HCO <sub>2</sub> Si	SiOCH <sub>2</sub> OSi	CH <sub>3</sub> OSi
2.00	0.46 (31%)	0.35 (24%)	0.65 (45%)
3.00	0.73 (31%)	0.60 (25%)	1.05 (44%)

<sup>a</sup> Conditions: CO<sub>2</sub> (1 atm), PhSiH<sub>3</sub> (2.00 or 3.00 mmol), cat. 1 (0.07 mol%), 55 °C, 18 h. <sup>b</sup> Determined by proton-coupled <sup>13</sup>C NMR using mesitylene as an internal standard. Product selectivity is shown in parentheses.

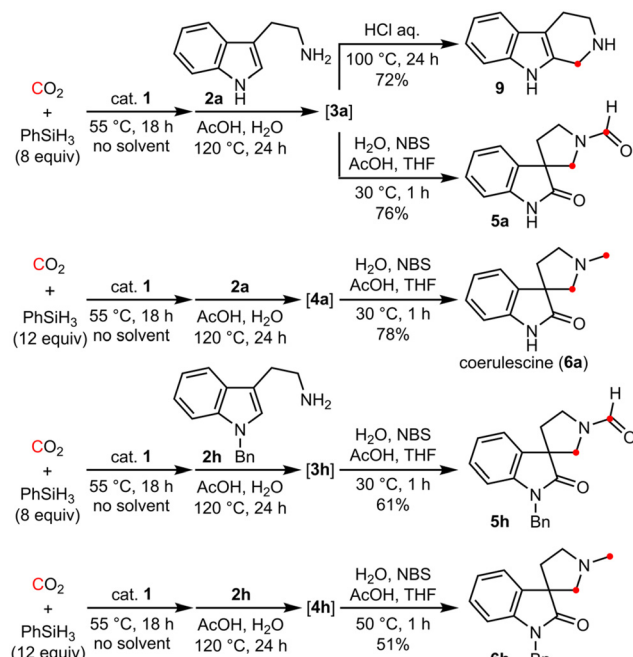


Scheme 5 Selected theoretical elementary reactions and TS structures for the formation of 3a and 4a at the B3LYP/6-31+G(d,p) level with the self-consistent reaction field method (H<sub>2</sub>O) at 393.15 K.  $\Delta G^\ddagger$  values and distances are shown in kcal mol<sup>−1</sup> and Å, respectively.  $\Delta G^\ddagger$  values are based on each elementary reaction.

be noted that the counterion in I2 for I3 can be either a formate or an acetate ion, whereas that for 11 must be a formate ion. In the actual experiments, the amount of added AcOH (3.5 mmol, 200  $\mu$ L) is much larger than that of the generated formic acid (up to 0.73 mmol), which likely leads to the preferential production of 9 rather than 11. The  $\Delta G^\ddagger$  value of the TS from 9 to 3a (10.7 kcal mol<sup>−1</sup>) is larger than that from 9 to 4a (6.4 kcal mol<sup>−1</sup>), which suggests that 4a is certainly formed preferentially when the reactive C1 intermediates are present in sufficient concentration (Scheme 5b). Several TSs are stabilized by water-involved hydrogen bonds, and the proton transfer is mediated by water; an example is P1\_TS, which involves dehydration.

### One-pot three-step reactions

Finally, we explored one-pot three-step reactions of 2 *via* 3 or 4 to demonstrate the potential of the aforementioned CO<sub>2</sub> conversions (Scheme 6). After the two-step reaction, hydrolysis of 3a with aqueous HCl gave tryptoline (9) in good yield (72%). When N-bromosuccinimide (NBS) was added in the third step,



**Scheme 6** One-pot three-step reactions for the synthesis of 5, 6, and 9.

formylated spiro[oxindole-pyrrolidine] **5a** was obtained in a high yield (76%). This method could also be applied to **4a**, and methylated spiro-compound **6a**, which is known as coerulescine, was obtained. In addition, the spiro-ring formation from the 1-benzyl analog **2h** to **5h** and **6h** was also achieved. These results further demonstrated the substantial potential of the one-pot synthesis strategy using mixtures of 1-catalyzed CO<sub>2</sub> reduction products.

## Conclusions

We have developed new deoxygenative dual CO<sub>2</sub> conversions in which CO<sub>2</sub> molecules were converted into different groups, methylene and *N*-formyl/*N*-methyl groups. Phenylsilane and a pentanuclear Zn complex acted as a highly efficient reductant and catalyst, respectively, and the reactions proceeded at atmospheric pressure without rare and harmful metals and solvents. The chemoselectivity of *N*-functionalization was switched by modifying only the amount of phenylsilane. These new CO<sub>2</sub> conversions will contribute greatly to the further development of CO<sub>2</sub> fixation.

## Author contributions

K. T. and T. E. conceived the project. H. M. and K. I. synthesized and characterized the compounds. K. T. conducted the DFT calculations. K. T. and T. E. wrote the initial draft of the manuscript, and all authors discussed the results and commented on the manuscript.

## Data availability

The data supporting the findings of this study are available in the ESI.†

## Conflicts of interest

There are no conflicts to declare.

## Acknowledgements

This work was supported by the Takahashi Industrial and Economic Research Foundation, the Yakumo Foundation for Environmental Science, and a Grant for the Promotion of Science and Technology in Okayama Prefecture by MEXT. We thank Dr Shigeki Mori (Ehime University) for the X-ray analyses. The computations were performed using RCCS, Okazaki, Japan (project: 24-IMS-C097).

## References

- 1 For selected reviews, see: (a) A. Tortajada, F. Juliá-Hernández, M. Börjesson, T. Moragas and R. Martin, *Angew. Chem., Int. Ed.*, 2018, **57**, 15948; (b) X. Jiang, X. Nie, X. Guo, C. Song and J. G. Chen, *Chem. Rev.*, 2020, **120**, 7984; (c) Y. Zhang, T. Zhang and S. Das, *Green Chem.*, 2020, **22**, 1800; (d) A. Modak, P. Bhanja, S. Dutta, B. Chowdhury and A. Bhaumik, *Green Chem.*, 2020, **22**, 4002; (e) D. A. Sable, K. S. Vadagaonkar, A. R. Kapdi and B. M. Bhanage, *Org. Biomol. Chem.*, 2021, **19**, 5725.
- 2 (a) M. Khandelwal and R. J. Wehmschulte, *Angew. Chem., Int. Ed.*, 2012, **51**, 7323; (b) R. J. Wehmschulte, M. Saleh and D. R. Powell, *Organometallics*, 2013, **32**, 6812; (c) Y. Li, T. Yan, K. Junge and M. Beller, *Angew. Chem., Int. Ed.*, 2014, **53**, 10476; (d) X. Zhang, S. Wang and C. Xi, *J. Org. Chem.*, 2019, **84**, 9744; (e) Q. Shi, H. Hu, M. Du, Y. Sun, Y. Li and Y. Li, *Org. Lett.*, 2023, **25**, 7100.
- 3 (a) X. Frogneux, E. Blondiaux, P. Thuéry and T. Cantat, *ACS Catal.*, 2015, **5**, 3983; (b) D.-Y. Zhu, L. Fang, H. Han, Y. Wang and J.-B. Xia, *Org. Lett.*, 2017, **19**, 4259; (c) C. Zhang, Y. Lu, R. Zhao, W. Menberu, J. Guo and Z.-X. Wang, *Chem. Commun.*, 2018, **54**, 10870; (d) M. Rauch, Z. Strater and G. Parkin, *J. Am. Chem. Soc.*, 2019, **141**, 17754; (e) W.-D. Li, J. Chen, D.-Y. Zhu and J.-B. Xia, *Chin. J. Chem.*, 2021, **39**, 614; (f) T. Murata, M. Hiyoshi, S. Maekawa, Y. Saiki, M. Ratanasak, J. Hasegawa and T. Ema, *Green Chem.*, 2022, **24**, 2385; (g) Z. Guo, J. Wu, X. Wei and C. Xi, *ChemSusChem*, 2025, **18**, e202401491; (h) A. Kumar, R. Gupta, V. Subramanyan and G. Mani, *Catal. Sci. Technol.*, 2025, **15**, 678.
- 4 W.-H. Wang, Y. Himeda, J. T. Muckerman, G. F. Manbeck and E. Fujita, *Chem. Rev.*, 2015, **115**, 12936.
- 5 S. Bontemps, *Coord. Chem. Rev.*, 2016, **308**, 117.



6 S. Desmons, J. Bonin, M. Robert and S. Bontemps, *Chem. Sci.*, 2024, **15**, 15023.

7 (a) F. J. Fernández-Alvarez and L. A. Oro, *ChemCatChem*, 2018, **10**, 4783; (b) Y. Zhang, T. Zhang and S. Das, *Green Chem.*, 2020, **22**, 1800; (c) R. A. Pramudita and K. Motokura, *ChemSusChem*, 2021, **14**, 281.

8 For recent examples of double carboxylations and related reactions, see: (a) Y. You, W. Kanna, H. Takano, H. Hayashi, S. Maeda and T. Mita, *J. Am. Chem. Soc.*, 2022, **144**, 3685; (b) M. Shigeno, I. Tohara, K. Sasaki, K. Nozawa-Kumada and Y. Kondo, *Org. Lett.*, 2022, **24**, 4825; (c) R. Giovanelli, L. Lombardi, R. Pedrazzani, M. Monari, M. Castiñeira, R. Carlos, S. López, G. Bertuzzi and M. Bandini, *Org. Lett.*, 2023, **25**, 6969; (d) C. Maeda, T. Cho, R. Kumemoto and T. Ema, *Org. Biomol. Chem.*, 2023, **21**, 6565; (e) F. Zhang, X.-Y. Wu, P.-P. Gao, H. Zhang, Z. Li, S. Ai and G. Li, *Chem. Sci.*, 2024, **15**, 6178; (f) Y.-Y. Gui, X.-W. Chen, X.-Y. Mo, J.-P. Yue, R. Yuan, Y. Liu, L.-L. Liao, J.-H. Ye and D.-G. Yu, *J. Am. Chem. Soc.*, 2024, **146**, 2919; (g) A. Brunetti, M. Garbini, G. Autuori, C. Zanardi, G. Bertuzzi and M. Bandini, *Chem. – Eur. J.*, 2024, **30**, e202401754; (h) H. Liu, M. Guo, M. Jia, J. Zhang and X. Xu, *Org. Lett.*, 2025, **27**, 778.

9 Y. Zhao, X. Liu, L. Zheng, Y. Du, X. Shi, Y. Liu, Z. Yan, J. You and Y. Jiang, *J. Org. Chem.*, 2020, **85**, 912.

10 S. Li, S. Nakahara, T. Adachi, T. Murata, K. Takaishi and T. Ema, *J. Am. Chem. Soc.*, 2024, **146**, 14935.

11 W. Xiong, X. Tan, H. Liu, B. Zhu, J. Zhao, J. Li, C. Qi and H. Jiang, *Sci. China: Chem.*, 2024, **67**, 841.

12 Q. Yan, J. Nan, R. Cao, L. Zhu, S. Liu, C. Liang and C. Zhang, *Org. Lett.*, 2025, **27**, 510.

13 K. Takaishi, B. D. Nath, Y. Yamada, H. Kosugi and T. Ema, *Angew. Chem., Int. Ed.*, 2019, **58**, 9984.

14 (a) K. Takaishi, H. Kosugi, R. Nishimura, Y. Yamada and T. Ema, *Chem. Commun.*, 2021, **57**, 8083; (b) K. Takaishi, R. Nishimura, Y. Toda, H. Morishita and T. Ema, *Org. Lett.*, 2023, **25**, 1370; (c) T. Ema, *Bull. Chem. Soc. Jpn.*, 2023, **96**, 693.

15 For recent reviews on *N*-formylation and *N*-methylation, see: (a) A. Tlili, E. Blondiaux, X. Frogneux and T. Cantat, *Green Chem.*, 2015, **17**, 157; (b) J.-Y. Li, Q.-W. Song, K. Zhang and P. Liu, *Molecules*, 2019, **24**, 182; (c) J. R. Cabrero-Antonino, R. Adam and M. Beller, *Angew. Chem., Int. Ed.*, 2019, **58**, 12820; (d) M. Hull and P. J. Dyson, *Angew. Chem., Int. Ed.*, 2020, **59**, 1002; (e) Z. Li, Z. Yu, X. Luo, C. Li, H. Wu, W. Zhao, H. Li and S. Yang, *RSC Adv.*, 2020, **10**, 33972; (f) G. Naik, N. Sarki, V. Goyal, A. Narani and K. Natte, *Asian J. Org. Chem.*, 2022, **11**, e202200270.

16 For recent examples, see: (a) H. Kobayashi, H. Hatakeyama, H. Nishimura, M. Yokota, S. Suzuki, Y. Tomabechi, M. Shirouzu, H. Osada, M. Mimaki, Y. Goto and M. Yoshida, *Nat. Chem. Biol.*, 2021, **17**, 335; (b) L. Ting, L. Shiru, D. Baiyun, L. Xiaofa, G. Yifan, R. R. Raphael, H. Jiadong, L. Long, Y. Peiyu, W. Ruotian, Z. Meng, G. Jinming, Y. Xia and C. Xin, *Eur. J. Med. Chem.*, 2024, **275**, 116624; (c) S. Eagon, J. T. Hammill, J. Bach, N. Everson, T. A. Sisley, M. J. Walls, D. Sierra, D. R. Pillai, M. O. Falade, A. L. Rice, J. J. Kimball, H. Lazaro, C. DiBernardo and R. K. Guy, *Bioorg. Med. Chem. Lett.*, 2024, **30**, 127502.

17 (a) C. Pellegrini, C. Strässler, M. Weber and H.-J. Borschberg, *Tetrahedron:Asymmetry*, 1994, **5**, 1979; (b) S. Edmondson, S. J. Danishefsky, L. Sepp-Lorenzino and N. Rosen, *J. Am. Chem. Soc.*, 1999, **121**, 2147.

18 (a) I. V. Efremov, F. F. Vajdos, K. A. Borzilleri, S. Capetta, H. Chen, P. H. Dorff, J. K. Dutra, S. W. Goldstein, M. Mansour, A. McColl, S. Noell, C. E. Oborski, T. N. O'Connell, T. J. O'Sullivan, J. Pandit, H. Wang, B. Wei and J. M. Withka, *J. Med. Chem.*, 2012, **55**, 9069; (b) H. Chen, P. Hua, D. Huang, Y. Zhang, H. Zhou, J. Xu and Q. Gu, *J. Med. Chem.*, 2023, **66**, 752.

19 Y. Hayashi, *Chem. Sci.*, 2016, **7**, 866.

20 Conformational analyses of **3a** and **4a** in solution were also carried out, see section 3 in the ESI.†

21 The volume of the  $^{13}\text{CO}_2$  balloon (0.3 L) was much smaller than that of the  $^{12}\text{CO}_2$  balloon (3.7 L), which probably led to the low yields of **3a'** and **4a'**.

22 The equivalents of formic acid and paraformaldehyde were roughly optimized on the basis of amounts of silyl formates and bis(silyl)acetals generated by **1**-catalyzed  $\text{CO}_2$  reduction, as discussed later (Table 2).

23 H. H. Cramer, B. Chatterjee, T. Weyhermüller, C. Werlé and W. Leitner, *Angew. Chem., Int. Ed.*, 2020, **59**, 15674.

